Article:
(2021) The structure of low-lying 1− states in 90,94Zr from (α,α′γ) and (p,p′γ) reactions. Physics Letters, Section B: Nuclear, Elementary Particle and High-Energy Physics. 136210. ISSN 0370-2693

https://doi.org/10.1016/j.physletb.2021.136210

Physics Letters B 816 (2021) 136210

Contents lists available at ScienceDirect

Physics Letters B

www.elsevier.com/locate/physletb

The structure of low-lying 1^- states in ^{90,94}Zr from $(\alpha, \alpha'\gamma)$ and $(p, p'\gamma)$ reactions

F.C.L. Crespi [a,b], A. Bracco [a,b,*], E.G. Lanza [c], A. Tamii [d], N. Blasi [b], F. Camera [a,b], O. Wieland [b], N. Aoi [d], D.L. Balabanski [e], S. Bassauer [f], A.S. Brown [g], M.P. Carpenter [h], J.J. Carroll [i], M. Ciemała [j], A. Czeszumska [d], P.J. Davies [g], V. Derya [k], L.M. Donaldson [l], Y.D. Fang [d], H. Fujita [d], G. Gey [d], H.T. Ha [d], M.N. Harakeh [d,m], T. Hashimoto [n], N. Ichige [o], E. Ideguchi [d], A. Inoue [d], J. Isaak [d,f], C. Iwamoto [p], D.G. Jenkins [g], T. Klaus [f], N. Kobayashi [d], T. Koike [o], M. Krzysiek [j], M.K. Raju [d], M. Liu [q], A. Maj [j], L. Morris [g], P. von Neumann Cosel [f], S. Noji [r], H.J. Ong [d], S.G. Pickstone [k], N. Pietralla [f], D. Savran [s], J.M. Schmitt [r], M. Spieker [t,k], G. Steinhilber [f], C. Sullivan [r,u,v], B. Wasilewska [j], M. Weinert [k], V. Werner [f], Y. Yamamoto [d], T. Yamamoto [d], R.G.T. Zegers [r,u,v], X. Zhou [q], S. Zhu [h], A. Zilges [k]

[a] *Dipartimento di Fisica dell'Università degli Studi di Milano, I-20133 Milano, Italy*
[b] *INFN, Sezione di Milano, I-20133 Milano, Italy*
[c] *INFN, Sezione di Catania, I-95100 Catania, Italy*
[d] *RCNP, Osaka Univ., Ibaraki, Osaka 5670047, Japan*
[e] *ELI-NP, Horia Hulubei National Institute for R&D in Physics and Nuclear Engineering, 077125 Bucharest-Magurele, Romania*
[f] *Institut für Kernphysik, Technische Universität Darmstadt, D-64289 Darmstadt, Germany*
[g] *Univ. of York, Dept. Phys., York YO10 5DD, N Yorkshire, England, United Kingdom*
[h] *Argonne Natl. Lab., Div. Phys, Argonne, IL 60439 USA*
[i] *CCDC/Army Research Laboratory, Adelphi, MD 20783, USA*
[j] *H. Niewodniczanski Institute of Nuclear Physics PAN, ul. Radzikowskiego 152, PL-31342 Krakow, Poland*
[k] *Institut für Kernphysik, Universität zu Köln, D-50937 Köln, Germany*
[l] *Univ. Witwatersrand, Sch Phys, ZA-2050 Johannesburg, South Africa*
[m] *University of Groningen, Zernikelaan 25, 9747 AA Groningen, the Netherlands*
[n] *Rare Isotope Science Project, Institute for Basic Science, Yuseong-gu, Daejeon 305-811, Republic of Korea*
[o] *Tohoku Univ, Dept Phys, Sendai, Miyagi 9808578, Japan*
[p] *Center for Nuclear Study, University of Tokyo, Tokyo 113-0033, Japan*
[q] *Institute of Modern Physics, Chinese Academy of Sciences, Lanzhou 730000, China*
[r] *National Superconducting Cyclotron Laboratory, Michigan State University, East Lansing, MI 48824, USA*
[s] *GSI Helmholtzzentrum für Schwerionenforschung GmbH, D-64291 Darmstadt, Germany*
[t] *Department of Physics, Florida State University, Tallahassee, FL 32306, USA*
[u] *Department of Physics and Astronomy, Michigan State University, East Lansing, MI 48824, USA*
[v] *Joint Institute for Nuclear Astrophysics: Center for the Evolution of the Elements, Michigan State University, East Lansing, MI 48824, USA*

ARTICLE INFO

Article history:
Received 26 October 2020
Received in revised form 8 March 2021
Accepted 9 March 2021
Available online 16 March 2021
Editor: B. Blank

Keywords:
Nuclear structure
Dipole excitation around neutron threshold
Inelastic scattering

ABSTRACT

The low-lying dipole strength in the ^{90,94}Zr nuclei was investigated via $(p, p'\gamma)$ at 80 MeV and $(\alpha, \alpha'\gamma)$ at 130 MeV. The experiments, made at RCNP, used the magnetic spectrometer Grand Raiden for the scattered particles and the array CAGRA with HPGe detectors for the γ-decay. For ^{94}Zr these are the first data for both reactions and for ^{90}Zr these are the first data with $(p, p'\gamma)$ and the first ones at high resolution for $(\alpha, \alpha'\gamma)$. The comparison of the present results for the two nuclei with existing (γ, γ') data shows that both nuclear probes produce an excitation pattern different than that of the electromagnetic probes.

DWBA calculations were made using form factors deduced from transition densities, based on RPA calculations, characterized by a strong neutron component at the nuclear surface. A combined analysis of the two reactions was performed for the first time to investigate the isoscalar character of the 1^- states in ^{90,94}Zr. The $(p, p'\gamma)$ cross section was calculated using values for the isoscalar electric dipole energy-

* Corresponding author at: Dipartimento di Fisica dell'Università degli Studi di Milano, I-20133 Milano, Italy.
E-mail address: Angela.Bracco@mi.infn.it (A. Bracco).

https://doi.org/10.1016/j.physletb.2021.136210

weighted sum rule (E1 ISEWSR) obtained from the $(\alpha, \alpha'\gamma)$ data. The isoscalar strength for ^{90}Zr was found to exhaust 20 $\pm$ 2.5% of the EWSR in the energy range up to 12 MeV. In case of ^{94}Zr, a strength of 9 $\pm$ 1.1% of the EWSR was found in the range up to 8.5 MeV.
Although an overall general description was obtained in the studied energy intervals, not all proton cross sections were well reproduced using the isoscalar strength from $(\alpha, \alpha'\gamma)$. This might suggest mixing of isoscalar and isovector components and that this mixing and the degree of collectivity are not the same for all the 1^- states below the particle binding energy.

The problem of understanding the features of the low-lying dipole strength at around and below the particle binding energy, commonly denoted as pygmy dipole resonance (PDR), is presently attracting particular interest (see, e.g., [1], [2]) and driving several experimental and theoretical efforts. The PDR notation for low-lying 1- states was introduced since their dipole strength is only few percent of the strength located in all nuclei in the Giant Dipole Resonance (GDR), at around 15-18 MeV. While the GDR can be well described as a collective dipole oscillation of all protons against all neutrons a general microscopic description of the PDR states is presently lacking. Although a simple proposed interpretation is based on the oscillation of neutrons at the nuclear surface against a core made by the other nucleons, the low-lying 1- states are expected to have a more complex structure depending on specific nuclear configurations. To unveil the properties of the PDR states it is important to know how much these states are excited by different probes. Multiple investigations are instrumental in this connection. By using different reactions employing hadronic probes of different types and electromagnetic probes one is expected to be sensitive to different regions on the nuclear volume and thus the comparison of the results provides indication on the nature of these states. In addition, to shed light on the dependence of specific nuclear configurations it is important to study different mass regions and isotopic chains. It has to be noted that there is interest in the PDR states beyond their nuclear-structure properties, because the presence of these dipole states has implications for astrophysical problems related to nucleosynthesis and the nuclear equation of state (see [3] for a review).
The results obtained so far, based on the comparison of the excitation of pygmy dipole states with both the electromagnetic and hadronic probes, reveal a structural splitting of the low-lying E1 strength. The states in the lower-energy region were shown to have isoscalar components larger than those of the states in the higher-energy region. In the case of ^{124}Sn ([4,5]) and ^{140}Ce ([6,7]), this splitting was clearly seen by comparing results from (γ, γ') with those obtained with two or more hadronic probes. For ^{124}Sn and ^{140}Ce, both $(\alpha, \alpha'\gamma)$ and $(^{17}O, ^{17}O'\gamma)$ show a consistent picture for this splitting. Moreover, for the ^{140}Ce nucleus, a recent work added relevant information, which was obtained with the $(p, p'\gamma)$ reaction [8]. In fact, while the cross section for the alpha and low-energy heavy-ion interaction is sensitive to the isoscalar component of the excited states, this is different in the case of proton scattering at a bombarding energy below 100 MeV where this selectivity is less distinct since proton scattering has also some sensitivity to isovector components and its surface-peaked interaction is less pronounced. The results for proton scattering off ^{140}Ce are consistent with an increase of the isovector character with excitation energy. In addition, from the measured cross sections, some evidence was found for a transitional region towards the IVGDR at higher energies. This work also underlines the importance of having additional data from proton scattering in that energy region.
This letter presents experimental work which advances the understanding of the isoscalar and isovector nature of the low-lying 1^- states by focusing on the two neutron rich nuclei ^{90,94}Zr. For these two nuclei (γ, γ') experiments have shown the presence of several 1^- states for which there is a need to have additional information on their excitation with hadron probes to describe their nature. In fact, up to now the experimental information based on hadronic probes on Zr isotopes relies on some data for ^{90}Zr from α scattering [9] and on $(^{17}O, ^{17}O'\gamma)$ [10], mainly limited to few excited states, while no data exist for ^{94}Zr. It has to be noted that the two nuclei ^{90,94}Zr, one being neutron closed shell and proton closed sub-shell and the other with additional four neutrons outside the neutron shell closure, provide a good testing ground for theory concerning predictions for isoscalar strength and of the role of the neutron excess outside the N=Z core in the structure of the PDR states. The existing data for ^{90}Zr indicate there is a need for further investigation in order to map the transition from states with "pygmy" like nature to the tail of the GDR. In addition, proton data are expected to play a role in clarifying the character of 1^- states. Moreover, the comparison between the two isotopes, for the first time investigated by using hadronic probes, could provide insight into the role of neutrons in the 1^- excitations.
The experiments were carried out at the Research Center for Nuclear Physics (RCNP), Osaka University. Beams of alpha particles and protons, at bombarding energies of 130 MeV and 80 MeV, respectively, were provided by the AVF cyclotron. Inelastically scattered particles (alphas or protons) were measured by employing the high-resolution spectrometer Grand Raiden (GR) [11]. In the used forward scattering mode, the GR spectrometer was placed at angles of 4.5 and 6.6 degrees, for the alpha and proton beams, respectively. The Grand Raiden Forward-mode beam line (GRAF) [12] was used to transport the unreacted beam to a well-shielded beam dump placed at 20 m downstream of the target. The full solid angle of the Grand Raiden spectrometer is 4 msr. Typical beam currents ranged from 4 to 10 nA, since the count rate in the focal plane detectors, which depends on the spectrometer angle, was kept rather constant during the data taking. Highly enriched self-supporting targets of ^{90,94}Zr with areal densities of 1.95 and 4 mg/cm^2, respectively, were used. The Grand Raiden spectrometer allowed measurements for both protons and alpha particles with energy resolutions between 60 and 100 keV (full width at half maximum, FWHM). A more detailed description of the coincidence setup at the Grand Raiden Spectrometer can be found in Ref. [12]. The γ rays emitted following the de-excitation of these target nuclei were detected using the clover-type HPGe detectors of the CAGRA array [13], placed around the target position. The CAGRA array consisted of 12 clover detectors, 8 of them were placed at an angle of 90 degrees with respect to the beam direction, while the remaining 4 clover detectors were placed at backward angles (135 deg). The distance between the target and the front face of the HPGe detectors was 208 mm for 10 clover detectors from Argonne National Laboratory (USA) and the Army Research Laboratory and 160 mm for 2 larger volume clover detectors from the Institute of Modern Physics (China). The energy resolution amounted to 20 keV at E_{ex} = 6.4 MeV. The total photo-peak efficiency was 0.0158 (0.00214) at 1332 keV (6.4 MeV).

The excitation energy was determined by the missing mass method from the energies of the scattered protons and α particles.

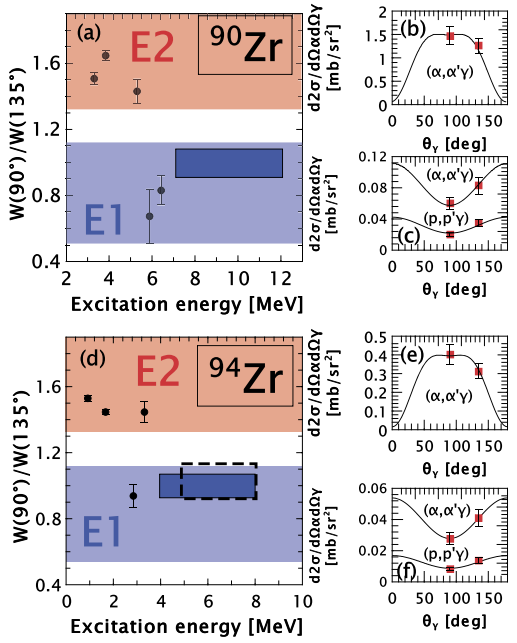

Fig. 1. The ratio of the measured yields at 90° and 135° for several transitions and the continuum regions (marked by horizontal blue bars) for ^{90}Zr (panel(a)) and ^{94}Zr (panel (d)) measured with the $(\alpha, \alpha'\gamma)$ reaction at 130 MeV. In both frames, the coloured regions refer to E2 (in red) and E1 (in blue) transitions types. The vertical size of the dark blue regions represents the statistical uncertainty related to the integral of counts. In panel (d) the rectangular region limited by dashed lines does not include the discrete transitions between 4.5 and 4.9 MeV. The measured and predicted γ angular correlations for selected discrete lines are shown panels (b), (c), (e), (f). The predictions were obtained with DWBA calculations. Panel (b) is for the 2186 keV E2 transition of ^{90}Zr and panel (c) is for the 6425 keV E1 transition of^{90}Zr. Panel (e) is for the 919 keV E2 transition of ^{94}Zr and panel (f) is for the 2846 keV E1 transition of^{94}Zr. The angular correlations for the $(p, p'\gamma)$ reaction, are characterised by a smaller anisotropy.

Ground-state γ-ray transitions from excited states were selected by setting energy gates with the condition $E_{ex} \approx E_\gamma$ for the excitation energy and energy of γ-ray transitions. This selection enhances the sensitivity to 1^- excited states due to their allowed E1 transition to the ground state. Random γ-coincidences were subtracted using the standard procedure in which a gate is set on the side of the prompt peak. The spectra extend up to around the neutron separation energy, Sn = 11.968 MeV and Sn = 8.219 MeV for ^{90}Zr and ^{94}Zr, respectively. The angular correlation of gamma rays and scattered particles was measured for two angular settings, 90° and 135°. The measured yields are shown in panels (b)(c)(e) and (f) of Fig. 1 for two transitions in each nucleus, one of quadrupole type and one of dipole type. The first 2^+ excited states of ^{90}Zr and ^{94}Zr are not present in the proton scattering spectra due to the acceptance of the magnetic spectrometer, set to measure the region of 1^- states. The γ angular distribution is sensitive to the multipole character of the transition as one can see in panels (b)(c)(e) and (f) of Fig. 1 where the data are compared with the corresponding calculated angular correlation. The theoretical angular correlation pattern was calculated with the program ANGCOR using the m-state population amplitudes obtained from DWBA calculations [14]. One can note that the anisotropy in the angular correlation is found to be larger in the case of alpha scattering.

The spin of the states which form a continuum distribution in the energy region of the PDR can be inferred by looking at the ratio between the number of counts measured at the two angles. This ratio is shown by the horizontal bars in Fig. 1 for the two nuclei ^{90}Zr and ^{94}Zr. In the figure, the red and blue regions correspond to the expected ratios for E2 and E1 transitions, respectively. The vertical size of these regions reflects the uncertainty in the spin alignment deduced from the angular correlation of few known discrete lines. The horizontal dark blue bars indicate the energy regions over which the counts were summed. For ^{94}Zr the horizontal bar limited by dashed lines does not contain discrete transitions. The vertical size of these bars gives the statistical uncertainty related to the integral of counts. The main finding is that the states in the energy regions 7-12 MeV for ^{90}Zr and 4-8 MeV for ^{94}Zr are primarily of electric dipole type.

The cross sections measured in this work are shown in panels (a) (b) (c) and (d) of Fig. 2 and are compared with data from (γ, γ') measurements, presented in panels (e) and (f) of Fig. 2 (from references [15] and [16]). In Fig. 2 the binning size of the data is 100 keV. Uncertainties of the present results are in the region of 10-20% in most cases, mainly dominated by statistical errors.

The counts in the known discrete peaks are indicated with full coloured bars (red and green) while the other grey bars correspond to the total measured counts and thus include the unresolved strength cross section. Similar to the findings in other nuclei, also for these two isotopes of Zr only the few lowest energy states are populated by all three reactions. However, for the lowest energy discrete states their population cross section with the (γ, γ') reaction is rather weak and this indicates that these states have a dominant isoscalar character. Note that also in the measurement for ^{90}Zr with the $(^{17}O, ^{17}O'\gamma)$ reaction [10] only the low-lying states up to 7 MeV were well populated.

The inspection of Fig. 2 indicates three clear distinctive features of the present data: i) in general the cross section for the $(p, p'\gamma)$ data is smaller than that of $(\alpha, \alpha'\gamma)$ similarly to the finding of [8] for ^{140}Ce; ii) a difference is present in the energy distribution of the cross section for the two hadronic probes as compared to the electromagnetic γ beam probe; iii) for the nucleus ^{90}Zr the cross section for $(p, p'\gamma)$ has a relative enhancement at around 9 MeV as compared to the $(\alpha, \alpha'\gamma)$ data.

One possible explanation of the additional cross sections in the $(p, p'\gamma)$ data around 9 MeV could be M1 excitations known to be favourably excited in proton scattering at forward angles [18]. Information on the M1 strength distribution in ^{90}Zr is available in Ref. [17] reporting the results of a reanalysis of the ^{90}Zr data of Ref. [19]. It was used, assuming 100% decay to the ground state, to estimate the contribution to the spectrum applying the conversion method described in Ref. [20]. The calculated cross section for the present bombarding energy and scattering angle is displayed in panel (c) of Fig. 2 with coloured (light green) bars. The uncertainty in the estimation of the M1 strength was deduced using the errors of the existing data and its average value is 19%. It varies from state to state and the standard deviation is 7%. The M1 contribution cannot account for the measured enhancement.

From the present results and from the ones in Ref. [8], it is clear that the proton and α scattering can be considered good isoscalar probes in the same way as light heavy-ion projectiles like ^{17}O [21,4,10,6] and ^{12}C [22]. We will try to make use of this isospin equivalence to extract relevant and valuable information about the low-lying dipole states in the two Zr isotopes. The reactions under study probe the nuclear surface. This can be inferred from a semiclassical model [23] where the trajectories are computed with classical equation of motion while the nuclear excitation is calculated according to quantum mechanics. The inelastic cross section is obtained by integrating over the impact parameters involved in the reaction. For each trajectory, the scattering angle as well as the distances of closest approach is obtained and therefore one can single out the values of the impact parameter that yield the measured scattering angles. In our case, the results of the inelastic cross section calculations show that the two projectiles, at the energies where the experiments were performed, are exploring the nuclear surface being the distance of closest approach close to the

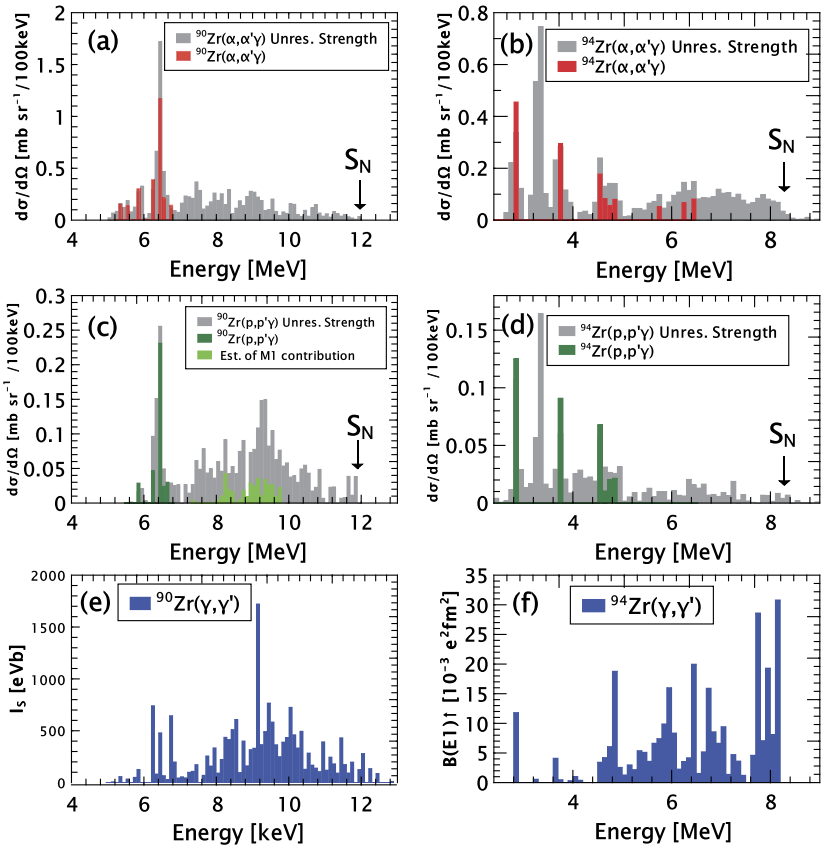

Fig. 2. Cross section for the excitation of dipole states from different reaction types for the nuclei ^{90}Zr and ^{94}Zr. Panels (a) and (b) are for the $(\alpha, \alpha'\gamma)$ reaction at 130 MeV, panels (c) and (d) are for the $(p, p'\gamma)$ reaction at 80 MeV, while panels (e) and (f) show (γ, γ') measurements from references [15] and [16]. The coloured bars correspond to discrete transitions while the grey bars correspond to the continuum regions in the present measurements. In panel (c) the estimated contribution from 1^+ states obtained using the measured M1 strength from [17] is shown in the grey area with light green bars.

nuclear radius for the proton scattering and close to the sum of the radii of the two reaction partner in the case of α scattering. Therefore the used reactions are well described within the DWBA approach. The radial form factors needed for the calculations of the inelastic scattering cross sections were constructed within the double folding approach (single folding for the proton scattering) with microscopic transition densities and the nucleon-nucleon M3Y interaction [24]. The transition densities employed here were calculated within the RPA approach. In panel (a) of Fig. 3, a typical transition density for the PDR is displayed for ^{90}Zr [25], calculated with a SGII interaction [26,27]. It shows at the surface the characteristic mixing of isoscalar and isovector character, i.e. the proton and neutron contributions are in phase inside the nuclear radius and only the neutron contribution is present at the nuclear surface. This feature has revealed its importance in the determination of the inelastic scattering cross section when it is calculated employing the DWBA approach [28]. Since the reactions measured in this work are expected to be probing the nucleus mainly around the surface, one expects that only the most external region of the transition density is responsible for the cross section. We have performed DWBA calculations for the 1^- state at 6.424 MeV in ^{90}Zr and that at 4.565 MeV in ^{94}Zr. For the optical potential the parameters deduced from existing elastic scattering data were used, see Refs. [29] and [30]. The Coulomb contribution was included in the DWBA calculations by using the $B_{em}(E1)$ deduced from the (γ, γ') measurements [15]. The Coulomb excitation cross section is in the range of 3-7 % of the total excitation and this is related to the isovector component of the states. The discrepancy between the theoretical cross section and the corresponding experimental value depends then on the nuclear contribution and the difference can be ascribed to the inaccurate value of the E1 ISEWSR [31] percentage for the considered state.

The DWBA calculations performed for the state at 6.424 MeV in ^{90}Zr were fitted to the data by varying the E1 ISEWSR strength of the state from the original theoretical value. In the case of the calculations corresponding to the transition density shown panel (a) of Fig. 3 the variation to fit the experiments was approximately 10%. We are aware of the fact that the nuclear cross section is not directly proportional to the $B_{is}(E1)$ but theoretical estimation has shown that it may be considered a plausible approximation [32]. It was noted that the excitation cross section is mainly of nuclear nature, where the cross section for Coulomb excitation is always smaller than 10%. The calculations were performed for the two reactions $(\alpha, \alpha'\gamma)$ and $(p, p'\gamma)$ on ^{90}Zr at 130 MeV and 80 MeV, respectively, and the deduced E1 ISEWSR values are plotted in panels (b) and (d) of Fig. 3. The blue bars correspond to the $(\alpha, \alpha'\gamma)$ reaction while the red bars to the $(p, p'\gamma)$ one. The error bars in the Fig. 3 reflect the statistical error. Similar calculations were made using form factors that employed transition densities obtained within the theoretical predictions from nuclear Energy Density Functional (EDF) (for a general review see Refs. [3] and [33]) based on different Skyrme functionals. In particular, for the ^{90}Zr nucleus, apart from the already mentioned SGII, the SAMi [34] and SkI3 [35] interactions were used. These interactions are representative of the numerous Skyrme interactions used in the literature and they all well describe the main features of the PDR states. Furthermore, they describe as well the main characteristics of the giant resonances and in particular of the IVGDR. For the ^{94}Zr nucleus, the SGII interaction was not considered because it does not include pairing effects.

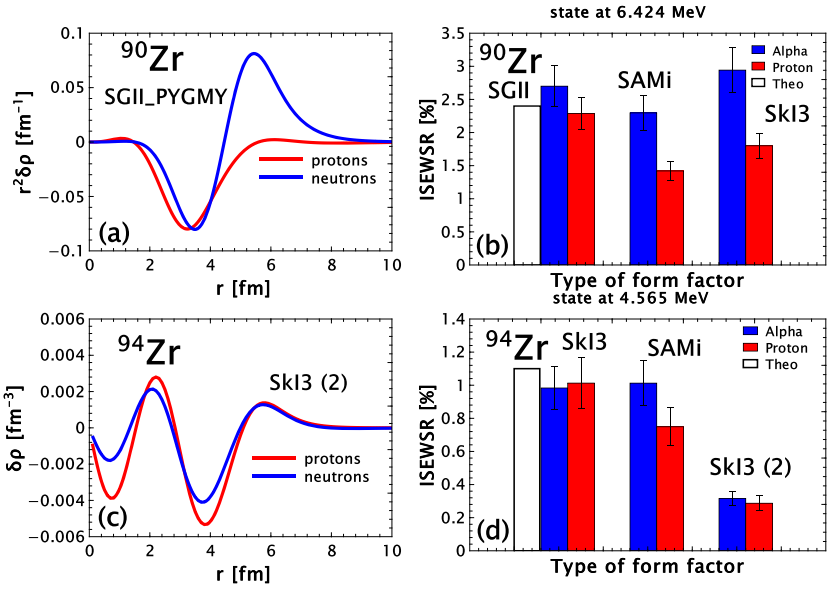

Fig. 3. Panels (a) and (c) show two predictions of the transition densities, one for the nucleus ^{90}Zr - typical of a pygmy dipole state - calculated with a SGII interaction (top left panel) and one for the nucleus ^{94}Zr - with no isospin mixing at the nuclear surface - calculated with a SkI3 interaction (bottom left panel) and indicated as SkI3(2). Panels (b) and (d) show the fraction of the ISEWSR strength deduced by comparing the data from α (blue bars) and proton (red bars) scattering with DWBA calculations using form factors calculated using transition densities obtained with different interaction within the EDF+RPA approach. Panel (b) refers to the 6424 keV state in ^{90}Zr and panel (d) is for the 4565 keV state in ^{94}Zr. For the SGII interaction for ^{90}Zr and the SkI3 interaction for ^{94}Zr the theoretical values of the ISEWSR strength are also shown with the empty bars. The bars denoted with SkI3(2) were obtained by using the transition densities on the bottom left panel while the ones indicated with SkI3 were obtained with transition densities that have a shape similar to the ones on the upper left panel.

In panel (b) of Fig. 3, the results for the value of ISEWSR(%) obtained as fit to the data are shown for the three mentioned interactions and for the state at 6.42 MeV in ^{90}Zr. The plotted quantity is thus ISEWSR(%) = ISEWSR(%)$_{th}$*(σ_{ex}/σ_{th}). For a given state, one expects to deduce the same value of the E1 ISEWSR strength independently of the used reaction. The fraction of the E1 ISEWSR deduced by comparing the data from alpha (blue bars) and proton (red bars) scattering with the theoretical DWBA calculations show that, for the case of the SGII interaction, the results are very similar. In addition, σ_{ex}/σ_{th} differs from 1 by approximately 10% only for the SGII interaction, while for the other two interactions, the difference is much larger up 70% or more. Therefore, we consider the calculation performed with transition density obtained using the SGII interaction to be the best one. The same type analysis was repeated for the dipole state at 4.565 MeV in ^{94}Zr and the results - shown in panel (d) of Fig. 3 - indicate that the best fit is obtained with the SkI3 interaction. One common feature of the transition densities for states around the particle binding energy here used is to have a neutron excess at the nuclear surface and this is true for all three interactions. This feature is typical of PDR states and is seen as related to isospin mixing. For states at higher excitation energy the transition densities for proton and neutrons have almost identical radial distribution at the surface. We considered interesting to make a calculation also using this type of transition density although it is related to higher energy states. We denote here with the label SkI3(2) the calculations using the transition density obtained with the SkI3 interaction for the states in ^{94}Zr at around 10 MeV having the proton and neutron radial distribution shown in panel (c) of Fig. 3. Inspection of panel (c) of Fig. 3 evidences that the proton and neutron components of this transition density are in phase also at the nuclear radius region. In this case the deduced percentage of the E1 ISEWSR is much smaller than the one obtained by using a transition density like the one in panel (a) of Fig. 3, which describes a state with a strong isospin mixing at the nuclear surface. In the supplementary material of this paper the transition density for the states in ^{94}Zr at around the binding energy based on the SkI3 interaction is given.

We used the best results obtained for α scattering to deduce for each of the two targets, from a fit, the value of the E1 ISEWSR strengths in the continuum region. In particular, for the form factor we employed the one based on the SGII interaction for ^{90}Zr and on the SkI3 interaction for ^{94}Zr. This choice takes into account two facts. One is that for the states at 6.424 MeV in ^{90}Zr and at 4.565 MeV in ^{94}Zr (see panels (b) and (d) of Fig. 3) it was found that the ISEWSR(%) values are similar for p and α scattering data. The second is that the ratio σ_{ex}/σ_{th} differs from 1 only by approximately 10%. Then, for the calculation of the $(p, p'\gamma)$ scattering cross section we made use of the proton form factor with a strength (namely the fraction of the ISEWSR) equal to that deduced from the α scattering analysis and without imposing any further normalisation. The form factors for the proton and alpha reactions are different as they result from transition densities single (proton) and double (alpha) folded with the same nucleon-nucleon M3Y interaction [24]. This procedure was applied for both nuclei ^{90}Zr and ^{94}Zr.

The calculated cross sections obtained for proton scattering are compared with the measurements in Fig. 4, for both the ^{90}Zr and ^{94}Zr nuclei. The error bars in this figure reflect the statistical error. In the case of ^{90}Zr the contribution of the M1 strength was taken into account. For ^{90}Zr, the calculations show some differences from the data and on average the difference is 0.12 mb/sr. The differences between the (p,p'γ) data and the calculation with the ISEWSR extracted from $(\alpha, \alpha'\gamma)$ data are probably reflecting the mixed character of the (p,p'γ) excitation. In particular, three energy bins show significant deviations between data and predictions, namely the two data points near 7 MeV have significantly stronger cross sections for the proton data, whereas only the last data point above 11.5 MeV shows a much smaller cross section for proton scattering. For this one cannot exclude that the M1 component, whose excitation cross section was estimated with calculations, was over or under estimated when subtracted from the data. The failure of reproducing the data for some states in ^{90}Zr with this simple analysis could indicate the presence of very dif-

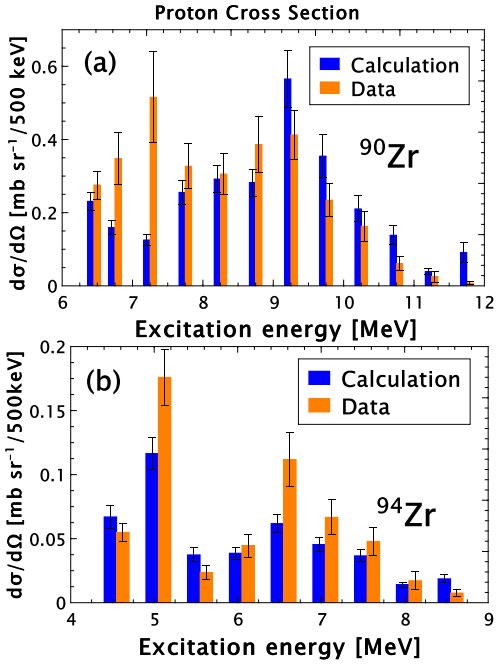

Fig. 4. The cross section measured with proton inelastic scattering at 80 MeV (integrated over a bin 0.5 MeV wide and in mb/sr) is shown with orange bars and the corresponding prediction, including as strength that determined by the $(\alpha, \alpha'\gamma)$ data, is shown with blue bars. Panel (a) is for the ^{90}Zr nucleus and panel (b) for the ^{94}Zr nucleus. The predictions are based, as described in the text, on DWBA calculations using values of the E1 EWSR strengths that were deduced from fitting of α scattering data of this work.

ferent structures and thus different isoscalar components probed by the two types of projectiles.

In the case of the ^{94}Zr the general trend of the data is described by these calculations in a rather satisfactory way with the exclusion of the points at 5 and 6.5 MeV for which discrepancies outside the error bars are found. For both nuclei the found discrepancies might be due to the fact that the assumption of a form factor to be the same over the entire excitation-energy region, which is considered here, is not fully appropriate. Moreover, the differences in between the (p,p'γ) data and the calculation using the ISEWSR extracted from the $(\alpha, \alpha'\gamma)$ data are probably reflecting the mixed character of the (p,p'γ) excitation. One can generally deduce that both reactions give a consistent picture of the 1^- states distribution as being a mixture of isoscalar and isovector type with a strong neutron contribution at the nuclear surface. It is also interesting to note that in the case of ^{94}Zr an increase of the B(E1) is found in the (γ, γ') data at around the neutron binding energy, while in contrast the nuclear excitation decreases in that region. This could be interpreted as due to a transition from isoscalar to isovector type for these states. In addition, it is found that the total isoscalar strength up to 12 MeV in ^{90}Zr is 20 $\pm$ 2.5% of the ISEWSR while that in ^{94}Zr is 9 $\pm$ 1.1%, albeit up to 8.5 MeV only. This seems to be in contrast to expectations since the ^{94}Zr nucleus is more neutron rich. This finding, although referring to a different excitation energy region, could be due to a smaller collectivity of these states. However one cannot exclude that the M1 contribution in ^{90}Zr is larger than that estimated and subtracted.

In summary the low-lying dipole strength in the two isotopes ^{90,94}Zr was measured using inelastic scattering of protons at 80 MeV and α particles at 130 MeV incident energies. For both proton and α scattering, the nuclear part is dominant for the excitation of the low-energy part of the pygmy dipole resonance. The size of the excitation cross section is overall satisfactorily reproduced using microscopic form factors corresponding to transition densities with a neutron contribution at the surface. These transition densities are characterised by protons and neutrons oscillating in phase in the inner region while at the nuclear surface the isovector and the isoscalar parts are of the same strength. The fraction of the isoscalar electric dipole EWSR strength was deduced by fitting the α scattering data with DWBA calculations and these deduced values were then used to calculate the proton cross section without any further normalisation. This coupled analysis of the two reaction data gives an overall acceptable description of the ^{90}Zr data and a more satisfactory description for ^{94}Zr data. It shows, from the found discrepancies, that the mixing of isoscalar and isovector components is not the same for all 1^- states below the particle binding energy. In addition, the (γ, γ') data show that there is an increase of the B_{em}(E1) strength around the neutron binding energy for the more neutron-rich isotope. In contrast, for the present case, the total isoscalar strength is found to decrease by going from ^{90}Zr to the more neutron rich ^{94}Zr. However, for the present measurements the energy region of 1^- states in ^{90}Zr extends to a larger interval (up to 12 MeV) as compared to that of ^{94}Zr, (up to 8.5 MeV) and thus one cannot exclude the presence of E1 transitions in ^{94}Zr at energies larger than 8.5 MeV, which are not here visible because of the high competition with neutron emission. By noting that the measured ISEWSR for ^{90}Zr is the sum of 8 $\pm$ 1% (for 5.5-8.5 MeV) with 12 $\pm$ 1.5 % (for 8.5-12 MeV), and that for ^{94}Zr up to 8.5 MeV a value 9 $\pm$ 1.1% was found, a simple extrapolation for ^{94}Zr at 8.5-12 MeV gives $\approx$ 14%. This expectation has to be taken with great caution, being very crude, and it has to be verified with data having statistics approximately 50 times larger than this one.

The present work provides a new surprising and interesting result that needs to be checked also in other nuclei and with additional improved modelling. It also indicates that the intrinsic underlying structure of the 1^- states plays a role.

Declaration of competing interest

The authors declare that they have no known competing financial interests or personal relationships that could have appeared to influence the work reported in this paper.

Acknowledgements

This work has been supported by the Italian Institute of Nuclear Physics (INFN). D.L.B. acknowledges support from the EU Development Fund and Competitiveness Operational Program for the ELI-NP Project Phase II (1/07.07.2016, COP, ID1334). This work was supported by the US National Science Foundation under Grants PHY-1565546 and PHY-1913554. J.I. and V. W. acknowledge support by the State of Hesse under grant "Nuclear Photonics" within the LOEWE program. V.W. acknowledge support by the German DFG under grant SFB 1245. This work was funded by the Deutsche Forschungsgemeinschaft (DFG, German Research Foundation) under Grant No. SFB 1245 (project ID 279384907) and Grant 510/7-1.

Appendix A. Supplementary material

Supplementary material related to this article can be found online at https://doi.org/10.1016/j.physletb.2021.136210.

References

[1] A. Bracco, E.G. Lanza, A. Tamii, Prog. Part. Nucl. Phys. 106 (2019) 360.
[2] D. Savran, T. Aumann, A. Zilges, Prog. Part. Nucl. Phys. 70 (2013) 210.
[3] X. Roca-Maza, N. Paar, Prog. Part. Nucl. Phys. 101 (2018) 96.
[4] L. Pellegri, et al., Phys. Lett. B 738 (2014) 519.
[5] J. Endres, et al., Phys. Rev. Lett. 105 (2010) 212503.
[6] M. Krzysiek, et al., Phys. Rev. C 93 (2016) 044330.
[7] D. Savran, et al., Phys. Rev. Lett. 97 (2006) 17502.

[8] D. Savran, et al., Phys. Lett. B 786 (2018) 16.
[9] T. Poelhekken, et al., Phys. Lett. B 278 (1992) 423.
[10] F.C.L. Crespi, et al., Phys. Rev. C 91 (2015) 024323.
[11] M. Fujiwara, et al., Nucl. Instrum. Methods Phys. Res., Sect. A 422 (1999) 484.
[12] N. Kobayashi, et al., Eur. Phys. J. A 55 (2019) 231.
[13] E. Ideguchi, et al., Nucl. Instrum. Methods Phys. Res., Sect. A (2021), in preparation for submission.
[14] M.N. Harakeh, L.W. Put, KVI internal report 67i, 1980, unpublished.
[15] R. Schwengner, et al., Phys. Rev. C 78 (2008) 064314.
[16] M. Zweidinger, Nuclear structure studies on medium-heavy mass nuclei using the method of nuclear resonance fluorescence, Ph.D. thesis, Technische Universität Darmstadt, 2016.
[17] G. Rusev, et al., Phys. Rev. Lett. 110 (2013) 022503.
[18] J. Birkhan, et al., Phys. Rev. C 93 (2016) 041302.
[19] C. Iwamoto, et al., Phys. Rev. Lett. 108 (2012) 262501.
[20] P. von Neumann-Cosel, A. Tamii, Eur. Phys. J. A 55 (2019) 110.
[21] F.C.L. Crespi, et al., Phys. Rev. Lett. 113 (2014) 012501.
[22] N.S. Martorana, et al., Phys. Lett. B 782 (2018) 112.
[23] E.G. Lanza, et al., Phys. Rev. C 84 (2011) 064602.
[24] G. Bertsch, et al., Nucl. Phys. A 284 (1977) 399.
[25] A. Bracco, F. Crespi, E. Lanza, Eur. Phys. J. A 51 (2015) 99.
[26] N.V. Giai, H. Sagawa, Phys. Lett. B 106 (1981) 379.
[27] N.V. Giai, H. Sagawa, Nucl. Phys. A 371 (1981) 1.
[28] E.G. Lanza, A. Vitturi, M.V. Andrés, Phys. Rev. C 91 (2015) 054607.
[29] V. Avrigeanu, et al., Phys. Rev. C 49 (1994) 2136.
[30] A. Nadasen, et al., Phys. Rev. C 23 (1981) 1023.
[31] M.N. Harakeh, A.E.L. Dieperink, Phys. Rev. C 23 (1981) 2329.
[32] E.G. Lanza, A. Vitturi, E. Litvinova, D. Savran, Phys. Rev. C 89 (2014) 041601(R).
[33] M. Bender, et al., Rev. Mod. Phys. 75 (2003) 121.
[34] X. Roca-Maza, G. Coló, H. Sagawa, Phys. Rev. C 86 (2012) 031306.
[35] P.G. Reinhard, H. Flocard, Nucl. Phys. A 584 (3) (1995) 467.